Seasonality of lower tropospheric stability in the Community Earth System Model

Daniel Watkins and Jennifer Hutchings

Oregon State University
College of Earth, Ocean, and Atmospheric Sciences

Key Results

- **Despite strong internal climate variability among CESM LE ensemble members, spread of lower tropospheric stability (LTS) within CESM LE is much smaller than spread within the CMIP5 or CMIP3 model ensembles**
- **The annual cycles of lower tropospheric stability in CESM LE and ERA-I differ both in phase and in amplitude**
- **Differences between ERA-I and CESM LE LTS, and in the relationship between LTS and sea ice concentration, are largest in regions with thicker sea ice**

Introduction

Lower tropospheric stability (LTS, defined here as $T_{850\ hPa} - T_{2m}$) has been linked to Arctic amplification through its influence on radiative cooling efficiency[1] and vertical propagation of surface fluxes[2]. Climate models show high disagreement in the Arctic, which indicates either (or both) high internal climate variability or uncertainty in climate physics[3]. Bias in Arctic LTS in climate models is a persistent problem[4,5,6]. Biases have been variously attributed to parameterization of boundary layer processes[5], representation of mixed phase clouds[6], and longwave radiation parameterization[7]. Here, we examine the role of interannual variability and differences in the seasonal cycle over sea ice surfaces using the Community Earth System Model Large Ensemble[8] (CESM LE) and the ECMWF Interim Reanalysis[9] (ERA-I).

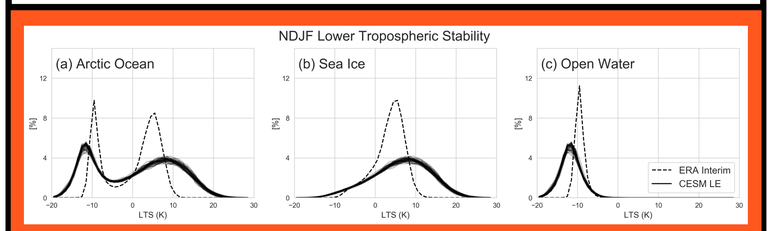

Figure 1. The bimodal LTS distribution over Arctic Ocean divides neatly into two unimodal distributions when split using a 15% sea ice concentration threshold. Thickness in the solid black line indicates differences between the 40 ensemble members of CESM LE. The form of the distribution is dependent on the averaging interval[4], here, we have binned individual monthly averages for Nov-Feb rather than using seasonal averages. Shorter averaging intervals generally results in a wider distribution.

Results

November-February LTS distributions over the Arctic Ocean have a bimodal distribution, as described in earlier studies[5,6]. Binning with the 15% SIC threshold reveals unimodal distributions over sea ice and open water domains, confirming that the stable (unstable) mode of LTS is the mode of the LTS distribution over sea ice (open water) as hown in FIgure 1. The mode of 40-year binned NDJF LTS distribution is 4.5 K in ERA-I and ranges from 5 to 11 K in CESM LE, with an average value of 8 K. Figure 2 compares the distribution of stable modes in ERA-I and CESM LE to values for CMIP5 and CMIP3 from the literature[5,6]. The distributions over the 1990-1999 interval and the 1980-2008 intervals are remarkably similar. In both cases, the spread within CESM LE is not large enough to explain the spread in the CMIP5 and CMIP3 ensembles.

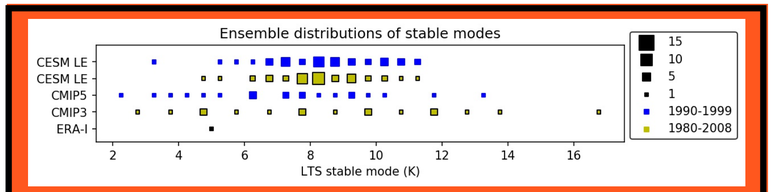

Figure 2. Distribution of winter (NDJF) stable modes for CESM LE and ERA-I compared with values for CMIP5 (blue) and CMIP3 (yellow). CMIP5 stable modes are from Pithan et al., (2014) and were computed for the period 1990-1999. CMIP3 stable modes are from Medeiros et al., (2011) and were computed for the period 1980-2008. (CMIP3). Size of squares indicates the number of models or ensemble members sharing the same value for the stable mode. For ERA-I, estimates over each time period were identical, so only a single square is displayed.

Investigation of the annual cycles of T_{850}, T_{2m}, and *LTS* reveals winter LTS peaking in Dec-Jan in ERA-I and in Mar-Apr in CESM LE (Figure 3). Compared with ERA-I, CESM LE is biased both at the surface and at altitude; however, it is at the surface that the seasonal cycle shows the strongest offset. Total cloud cover is biased high in late summer, while low cloud cover is biased high Feb-Oct. Low clouds typically reflect longwave radiation toward the surface, increasing surface temperatures. Absence of winter liquid clouds[10] in CESM may be to blame for the winter cold T_{2m} bias.

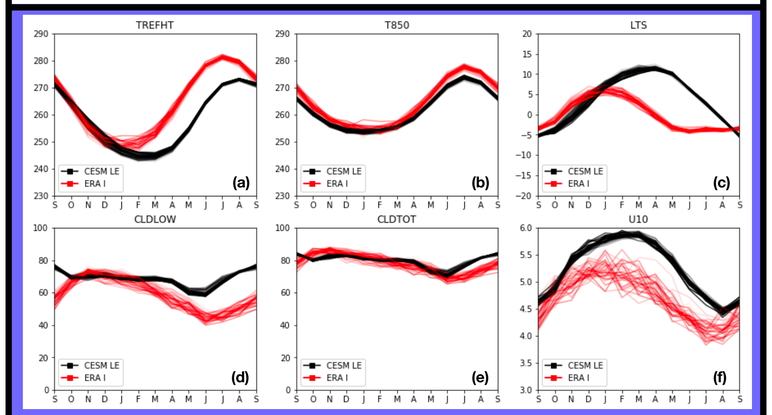

Figure 3. Annual cycle for (a) 2-meter temperature, (b) temperature at 850 hpa, (c) lower tropospheric stability, (d) low cloud fraction, (e) total cloud fraction, and (f) 10-meter wind speed. Each line represents one year between January 1979 and December 2018, with line opacity increasing in time. Red lines are from the ERA-Interim reanalysis, while black lines are from the CESM-LE ensemble average.

Strong biases in LTS persist from mid-winter to the beginning of fall. Satellite observations show a linear relationship relationship between mean annual sea ice concentration and Dec-Feb LTS[11]. Figure 4 shows that LTS/SIC relationship is tighter and steeper in CESM LE compared with ERA-I. The largest difference is in the region with >90% mean annual sea ice concentration. In Figure 5, LTS gradients for Jan-Apr over sea ice mirror gradients of sea ice thickness (not shown).

Next Steps

- Decomposing relationship of sea ice and LTS in NCEP CFSR
- Regional climate model (RASM): effect of higher grid resolution and usage of WRF instead of CAM
- AIRS-derived satellite LTS annual cycle
- Comparison with CESM2

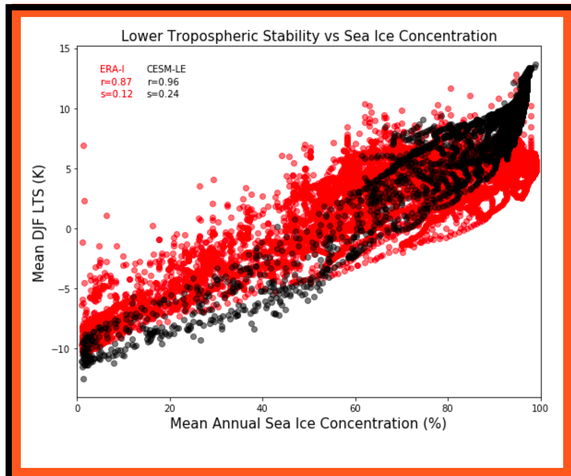

Figure 4. Correspondence between DJF LTS and annual sea ice concentration for CESM LE (black) and ERA-I (red). Linear regression coefficient significant at the 99% confidence level. Based on analysis in Pavelsky et al., (2011), who examined LTS/SIC relationships using AIRS clear-sky LTS and NSIDC sea ice concentrations, finding r=0.88 and s=0.13. CESM-LE shows a tighter correlation with a steeper slope.

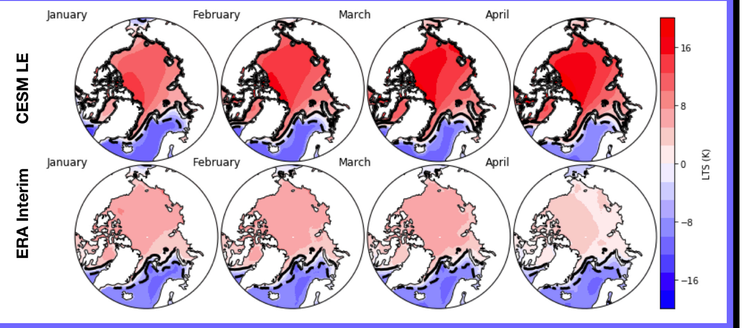

Figure 5. Average LTS in CESM LE (top) and ERA-I (bottom) for Jan-Apr. The dashed black line indicates the 15% SIC contour, while the solid black line indicates 90% SIC.

Data and computational acknowledgements

Monthly mean output from the Community Earth System Model Large Ensemble[3] (CESM LE) and the ECMWF Interim Reanalysis[4] (ERA-I) for the time period 1979-2018 were obtained from the NCAR Research Data Archive. Analysis was performed on NCAR's Casper computer. Model-level data was interpolated to the 850 hPa pressure level using `PyNgl`. Area-weighed means and histograms were computed using `xarray` and `numpy`, respectively. We used 0.5 K bins for histograms and computed the position of the LTS stable mode using the peak of the histogram-derived density. Maps were made using `cartopy` and plots using `matplotlib` and `seaborn`. Linear regression coefficients were computed with `scipy.stats`.

References

1. Bintanja, R., Graversen, R. G., & Hazeleger, W. (2011). Arctic winter warming amplified by the thermal inversion and consequent low infrared cooling to space. *Nature Geoscience*, *4*(11), 758–761.
2. Bintanja, R., van der Linden, E. C., & Hazeleger, W. (2012). Boundary layer stability and Arctic climate change: A feedback study using EC-Earth. *Climate Dynamics*, *39*(11), 2659–2673.
3. Swart, N. C., Fyfe, J. C., Hawkins, E., Kay, J. E., & Jahn, A. (2015). Influence of internal variability on Arctic sea-ice trends. Nature Climate Change, 5(2), 86–89. https://doi.org/10.1038/nclimate2483
4. Boe, J., Hall, A., & Qu, X. (2009). Current GCMs' Unrealistic Negative Feedback in the Arctic. *J. Climate*, *22*(17), 4682–4695.
5. Medeiros, B., Deser, C., Tomas, R. A., & Kay, J. E. (2011). Arctic Inversion Strength in Climate Models. Journal of Climate, 24, 4733–4740.
6. Pithan, F., Medeiros, B., & Mauritsen, T. (2014). Mixed-phase clouds cause climate model biases in Arctic wintertime temperature inversions. *Climate Dynamics*, *43*(1–2), 289–303.
7. Barton, N. P., Klein, S. A., & Boyle, J. S. (2014). On the contribution of longwave radiation to global climate model biases in arctic lower tropospheric stability. *Journal of Climate*, *27*(19), 7250–7269.
8. Kay, J. E., Deser, C., Phillips, A., Mai, A., Hannay, C., Strand, G., … Vertenstein, M. (2015). The community earth system model (CESM) large ensemble project: A community resource for studying climate change in the presence of internal climate variability. *Bulletin of the American Meteorological Society*, *96*(8), 1333–1349.
9. Dee, D. P., Uppala, S. M., Simmons, A. J., Berrisford, P., Poli, P., Kobayashi, S., … Vitart, F. (2011). The ERA-Interim reanalysis: Configuration and performance of the data assimilation system. *Quarterly Journal of the Royal Meteorological Society*, *137*(656), 553–597.
10. Pithan, F., Ackerman, A., Angevine, W. M., Hartung, K., Ickes, L., Kelley, M., … Zadra, A. (2016). Select strengths and biases of models in representing the Arctic winter boundary layer over sea ice: the Larcform 1 single column model intercomparison. *Journal of Advances in Modeling Earth Systems*, *8*, 1345–1357.
11. Pavelsky, T. M., Boe, J., Hall, A., & Fetzer, E. J. (2011). Atmospheric inversion strength over polar oceans in winter regulated by sea ice. Climate Dynamics, 36(5–6), 945–955.